Open access • Journal Article • DOI:10.1111/J.1460-9568.2004.03428.X

Segregation of two endocannabinoid-hydrolyzing enzymes into pre- and postsynaptic compartments in the rat hippocampus, cerebellum and amygdala.

Attila I. Gulyás, Benjamin F. Cravatt, Michael H. Bracey, Thien P. Dinh ...+3 more authors

Institutions: Hungarian Academy of Sciences, Scripps Research Institute, University of California, Irvine, University of Naples Federico II

Published on: 01 Jul 2004 - European Journal of Neuroscience (Blackwell Science Ltd)

Topics: Fatty acid amide hydrolase, Granule cell, Purkinje cell, Neuropil and Cerebellum

Title

Segregation of two endocannabinoid-hydrolyzing enzymes into pre- and postsynaptic compartments in the rat hippocampus, cerebellum and amygdala.

Journal

The European journal of neuroscience, 20(2)

ISSN

0953-816X

Authors

Gulyas, AI
Cravatt, BF
Bracey, MH
et al.

Publication Date

2004-07-01

DOI

10.1111/j.1460-9568.2004.03428.x

European Journal of Neuroscience, Vol. 20, pp. 441–458, 2004

Segregation of two endocannabinoid-hydrolyzing enzymes into pre- and postsynaptic compartments in the rat hippocampus, cerebellum and amygdala

A. I. Gulyas,[1] B. F. Cravatt,[2] M. H. Bracey,[2] T. P. Dinh,[3] D. Piomelli,[3] F. Boscia[4] and T. F. Freund[1]
[1]Institute of Experimental Medicine, Hungarian Academy of Sciences, Budapest, PO Box 67, H-1450, Hungary
[2]The Scripps Research Institute, 10550 N. Torrey Pines Road, La Jolla, CA 92037, USA
[3]Department of Pharmacology, University of California Irvine, Irvine, CA 92697, USA
[4]Department of Neuroscience, Section of Pharmacology, School of Medicine, University of Naples 'Federico II', Via Pansini 5, 80131-Naples, Italy

Keywords: 2-AG, anandamide, Ca^{2+} stores, electron microscopy, inhibitory cells, interneurons

Abstract

Fatty acid amide hydrolase (FAAH) and monoglyceride lipase (MGL) catalyse the hydrolysis of the endocannabinoids anandamide and 2-arachidonoyl glycerol. We investigated their ultrastructural distribution in brain areas where the localization and effects of cannabinoid receptor activation are known. In the hippocampus, FAAH was present in somata and dendrites of principal cells, but not in interneurons. It was located mostly on the membrane surface of intracellular organelles known to store Ca^{2+} (e.g. mitochondria, smooth endoplasmic reticulum), less frequently on the somatic or dendritic plasma membrane. MGL immunoreactivity was found in axon terminals of granule cells, CA3 pyramidal cells and some interneurons. In the cerebellum, Purkinje cells and their dendrites are intensively immunoreactive for FAAH, together with a sparse axon plexus at the border of the Purkinje cell/granule cell layers. Immunostaining for MGL was complementary, the axons in the molecular layer were intensively labelled leaving the Purkinje cell dendrites blank. FAAH distribution in the amygdala was similar to that of the CB_1 cannabinoid receptor: evident signal in neuronal somata and proximal dendrites in the basolateral nucleus, and hardly any labelling in the central nucleus. MGL staining was restricted to axons in the neuropil, with similar relative signal intensities seen for FAAH in different nuclei. Thus, FAAH is primarily a postsynaptic enzyme, whereas MGL is presynaptic. FAAH is associated with membranes of cytoplasmic organelles. The differential compartmentalization of the two enzymes suggests that anandamide and 2-AG signalling may subserve functional roles that are spatially segregated at least at the stage of metabolism.

Introduction

The identity and localization of cannabinoid receptors as well as their endogenous ligands have been recently reported (Devane *et al*., 1988,1992; Matsuda *et al*., 1990; Stella *et al*., 1997). In the hippocampus and cerebellum, cannabinoid receptors subtype 1 (CB_1) were shown to mediate depolarization-induced suppression of inhibition and excitation (Kreitzer & Regehr, 2001a,b; Wilson & Nicoll, 2001; Ohno-Shosaku *et al*., 2001), suggesting that endocannabinoids act as retrograde modulators of synaptic signalling.

Activity-dependent release of endocannabinoids from hippocampal pyramidal and cerebellar Purkinje cells activate cannabinoid receptors located on excitatory and inhibitory axon terminals (Katona *et al*., 1999), and reduce γ-aminobutyric acid (GABA; Hajos *et al*., 2000; Hoffman & Lupica, 2000) and glutamate (Shen *et al*., 1996; Misner & Sullivan, 1999) release. Recent experiments suggest that retrograde modulation of glutamatergic and GABAergic transmission may involve different cannabinoid receptors. In the hippocampus, CB_1 is selectively located in GABAergic axons (Katona *et al*., 1999), whereas glutamate release is regulated by a so far unidentified receptor (Hajos *et al*., 2001).

The two well-established endogenous cannabinoids are anandamide (the ethanolamide of arachidonic acid) and *sn*-2-arachidonoyl-glycerol (2-AG). A phospholipase D/N-acetyltransferase-dependent pathway is responsible for the synthesis of anandamide (Cadas *et al*., 1997), while phospholipase C and diacylglycerol lipase are thought to be involved in the synthesis of 2-AG (Stella *et al*., 1997). Electrical stimulation of hippocampal slices increases the levels of 2-AG (Stella *et al*., 1997). In cultured cortical neurons, activation of *N*-methyl-D-aspartate receptors increases 2-AG levels but has no effect on anandamide formation, which requires instead the simultaneous activation of *N*-methyl-D-aspartate and α-7 nicotinic receptors (Stella & Piomelli, 2001).

Fatty acid amide hydrolase (FAAH) and monoglyceride lipase (MGL) have been identified as degrading enzymes of endogenous cannabinoids. Breakdown of 2-AG has been attributed to MGL (Dinh *et al*., 2002). In contrast, the experiments demonstrating that FAAH –/– mutant mice cannot metabolize anandamide (Cravatt *et al*., 2001) while 2-AG hydrolysis is preserved (Lichtman *et al*., 2002) suggest that FAAH is the main anandamide-metabolizing enzyme.

The distribution of CB_1 receptors in different areas of the brain has been outlined using radioligand binding (Herkenham *et al*.,

Correspondence: Dr A. I. Gulyas, as above.
E-mail: gulyas@koki.hu

Received 19 March 2004, revised 7 April 2004, accepted 13 April 2004

doi:10.1111/j.1460-9568.2004.03428.x

1990; Mailleux & Vanderhaeghen, 1992). The receptor is expressed in several brain areas with a characteristic pattern, often associated with identified cell types. However, no data are available yet on the cellular and subcellular localization of the enzymes that catalyse endocannabinoid hydrolysis, except for low-resolution light microscopic descriptions of FAAH (Egertova *et al*., 2003) and MGL (Dinh *et al*., 2002). The brain distribution of FAAH and MGL mRNA have been reported (Thomas *et al*., 1997; Dinh *et al*., 2002). Identifying the exact sites of elimination of anandamide and 2-AG may shed light on their functional roles and help to understand their mechanisms of deactivation in the intact brain. Therefore, the present study investigated the distribution of FAAH and MGL at the light and electron microscopic levels in three brain regions in which endocannabinoid signalling has been shown to play important roles: the hippocampus, amygdala and cerebellum. The presence of the enzymes in different marker-containing, functionally distinct interneuron types has also been studied in the hippocampus using double-labelling methods.

Materials and methods

Handling and perfusion of animals

Experiments were performed according to the guidelines of the Institutional Ethical Codex & the Hungarian Act of Animal Care & Experimentation (1998, XXVIII, Section 243/1998), which is in full agreement with the regulation of animal experiments in the European Union. All efforts were made to reduce the number of animals used.

For the localization of FAAH, 13 adult (250 g) male Wistar rats (Charles-River, Hungary) and four adult mice (two FAAH +/+ and two FAAH –/–) were perfused under equithesine anaesthesia (chlornembutal 0.3 mL/100 g), first with physiological saline (1 min) and then with a fixative containing 1% glutaraldehyde (TAAB, UK), 3% paraformaldehyde (TAAB, UK) and 0.05% picric acid in 0.1 M phosphate buffer (PB) for 30 min. For the MGL immunostainings, six rats were perfused with the fixative described above.

After fixation, the dorsal hippocampi were dissected and sectioned on a vibratome at 60 μm. Following extensive washes in PB, the sections were immersed in a mixture of 25% sucrose and 10% glycerol in 0.1 M PB, and freeze-thawed over liquid nitrogen to increase the penetration of antisera.

Pre-embedding immunostaining

Sections were washed three times for 30 min between each step. All the washing steps and the dilution of the antisera were carried out in 50 mM Tris-buffered saline (pH 7.4). The sections were incubated first in 2% bovine serum albumin (for 45 min, Sigma), then in one of the primary antibodies for 2 days at 4°. Rabbit anti-FAAH antisera were generated against FAAH-GST (glutathione S-transferase) fusion protein (Patricelli *et al*., 1998; anti-FAAH, used in 1 : 1500), the other directed against a native, 6X-His tagged truncation of FAAH purified as described in Bracey *et al*. (2002; anti-FAAH-ΔTM, used in 1 : 3000). The rabbit anti-MGL serum (Dinh *et al*., 2002) was used in 1 : 5000 dilution. Following the primary antisera, sections for immunoperoxidase reaction were incubated in biotinylated goat anti-rabbit IgG (1 : 300 Vector Laboratories, CA, USA, 4 h) and then in Elite ABC (1 : 400 Vector Laboratories, 3 h). The peroxidase reaction was developed by 3,3′-diaminobenzidine–4HCl (DAB, Fluka Sigma-Aldrich, Hungary) as a chromogen. After the final washes in PB, the sections were treated with 1% OsO_4 for 1 h, dehydrated in ethanol and embedded in Durcupan (Fluka Sigma-Aldrich).

For pre-embedding immunogold staining against FAAH, the sections were incubated in anti-FAAH-ΔTM antiserum (1 : 500, 2 days) followed by 1 nm gold conjugated goat anti-rabbit antibody (1 : 50, overnight incubation, Amersham, UK). Gold labelling was intensified using the R-Gent silver intensification kit (Aurion, Wageningen, the Netherlands). Sections were then osmicated (0.5% OsO_4, 30 min, 4 °C), dehydrated and embedded in Durcupan.

Double pre-embedding immunostaining

We aimed to study the co-localization of MGL and cholecystokinin (CCK) at the ultrastructural level. For this purpose, the following staining procedure was carried out: the sections were incubated in a mixture of rabbit anti-MGL (1 : 5000) and mouse anti-CCK (1 : 2000, CURE, Digestive Diseases Research Center, USA) antibodies for 2 days. This was followed by incubation in gold conjugated goat anti-mouse (1 : 50, overnight incubation, Aurion) and silver intensification (see above) of the gold particles to detect CCK. Biotinylated goat anti-rabbit IgG (1 : 300, 4 h, Vector Laboratories) and Elite ABC (1 : 400, 3 h, Vector Laboratories), followed by developing of the reaction with DAB was used to visualize MGL.

Double-immunofluorescent staining

Incubation of sections in 2% bovine serum albumin (see above) was followed by mixtures of primary antibodies for overnight incubation: rabbit anti-FAAH-ΔTM (1 : 500) was mixed with mouse anti-GABA (1 : 75, Szabat *et al*., 1992) or mouse anti-GAD65 (1 : 200, CHEMICON International, Temecula, USA) or mouse anti-parvalbumin (PV; 1 : 1000, Fluka Sigma-Aldrich) or mouse anti-calbindin (1 : 6000, Fluka Sigma-Aldrich) or mouse anti-CCK (1 : 5000, CURE, Digestive Diseases Research Center) or mouse anti-calretinin (1 : 1000, SWANT, Bellinzona, Switzerland). After repeated washes in Tris-buffered saline, the sections were incubated in mixtures of fluorescent-labelled secondary antibodies for 2 h. Against the FAAH antibody we used goat anti-rabbit-FITC (1 : 50, Jackson ImmunoResearch Laboratories, Pennsylvania, USA), that was mixed with goat anti-mouse-Cy3 (1 : 200, Jackson ImmunoResearch Laboratories) to label the other markers. The sections were then washed in Tris-buffered saline, transferred onto microscope slides and covered with Vectashield (Vector Laboratories). The sections were evaluated using a Zeiss (Germany) Axioplan2 microscope with filters for FITC (excitation BP450–490, emission BP515–565) and for Cy3 (excitation BP546/12, emission LP590).

Controls

Antisera specificity was confirmed by the laboratories of origin (Patricelli *et al*., 1998; Bracey *et al*., 2002; Dinh *et al*., 2002). Controls of the methods in the present experiments included replacement of the primary antisera with normal serum (1 : 200). In the case of the FAAH antibodies, specificity was verified by the fact that no staining could be seen in the FAAH-KO animals. In case of MGL the antibody was preabsorbed with the immunizing peptide (SSPRRTPQNVPYQDL). In the latter cases no signal was visible apart from a faint background limited to the surface of the sections. In double-labelled sections the pattern of immunoreactivity for both antigens was identical to that seen in single-stained material.

Quantitative analysis of subcellular distribution of FAAH

To ensure an unbiased estimation of the relative distribution of silver-intensified immunogold particles over different cellular compartments, a random sampling was made in selected areas of the hippocampus and cerebellum. High-magnification non-overlapping electron micrographs were taken randomly, using a MegaViev II CCD camera, from the following areas: hippocampus CA1 area str. radiatum, cerebellum str. moleculare, cerebellum Purkinje cells bodies. Because we wanted to know the relative distribution of gold particles among different compartments and the size of the gold particles is small compared to the area of the electron micrographs, no special stereological sampling method had to be used. For the counting we identified the position of each gold particle over (or next to) the following elements: cell surface membrane, endoplasmic reticulum, mitochondrion outer membrane, stacked saccules of smooth endoplasmic reticulum (in the cerebellum only) and cytoplasm. A particle was assigned to one of the membrane-delineated compartments if the particle was within 40 nm from a membrane (we chose this value because it is the average diameter of a silver-intensified gold particle). If a particle was further away it was assigned to the cytoplasm.

Results

Two antibodies were used to visualize the distribution of FAAH at the cellular and subcellular levels. Anti-FAAH was raised against FAAH-GST fusion protein, while the anti-FAAH-ΔTM was raised against a native, 6X-His tagged truncation of FAAH. Staining with the two antibodies resulted in identical labelling pattern, as shown in Fig. 1 in the hippocampus. The specificity of the FAAH antibodies was verified by immunostaining hippocampal sections from FAAH-KO mice. No signal could be detected with either of the antibodies (Fig. 1C and D). Because the anti-FAAH-ΔTM antibody worked best at a higher dilution than the anti-FAAH and gave a signal with somewhat lower background, in the rest of the study we used the anti-FAAH-ΔTM for immunostaining at the light and electron microscopic levels. In the case of FAAH both the DAB and the pre-embedding gold visualization methods were employed for precise subcellular localization of the protein. In the case of MGL, ultrastructural localization was investigated with DAB alone. Immunogold localization was not required as, opposed to FAAH, MGL is a cytosolic protein (Dinh *et al*., 2002).

Light microscopical distribution of FAAH in the hippocampus

The distribution of FAAH in pyramidal cells of the hippocampus has been described recently at the light microscopic level (Tsou *et al*., 1998b; Egertova *et al*., 2003) using the same antisera. The present study confirmed these results, which will be described only briefly. Attention will be focused on our novel observations, namely the presence of FAAH immunoreactivity in different interneuron types and the subcellular distribution of FAAH at the electron microscopic level using immunogold labelling.

It is evident already at low magnification (Fig. 1A and B) that FAAH is associated with principal neurons of the hippocampus, as the principal cell layers are distinctively immunoreactive. At higher magnification a fine-grained, reticular immunoperoxidase reaction characterizes the immunostaining in the principal cell cytoplasm, proximal dendrites, as well as in the neuropil. In the CA1 area, the signal is present in all layers (Fig. 2A). The strongest signal is visible in the cytoplasm of the pyramidal cells, no labelling can be detected in the nucleus. Distinctly labelled by FAAH immunoreactivity, the apical and basal pyramidal cell dendrites can be followed for considerable distances. The intensity of the labelling decreases distally from str. pyramidale, most probably due to pyramidal cell dendrites forming thinner, secondary branches that are covered with dendritic spines. In the distal two-thirds of str. oriens, the upper half of str. radiatum and the str. lacunosum-moleculare, a fine-grained neuropil staining is displayed. In the CA3 area the distribution of FAAH is very similar to

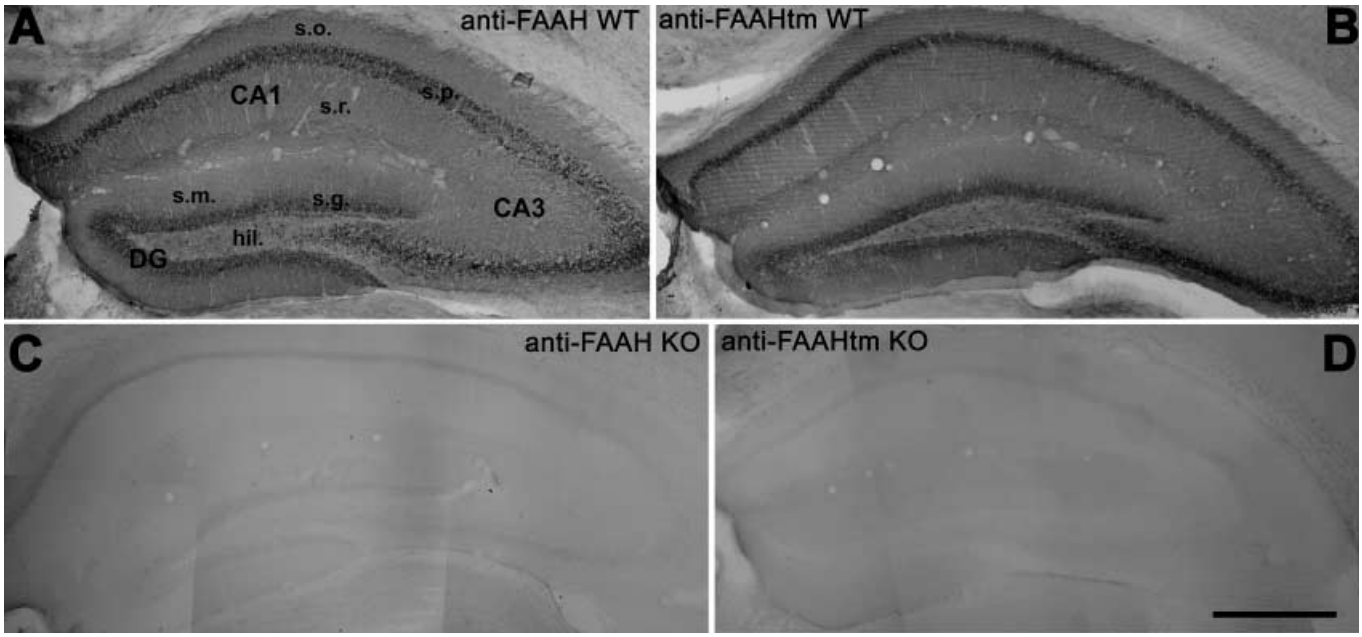

FIG. 1. Specificity of the fatty acid amide hydrolase (FAAH) antibodies used. Two antibodies were raised: one against a FAAH-GST fusion protein (anti-FAAH), the other against 6X-His tagged truncation of FAAH (anti-FAAH-ΔTM). As shown in A and B, the two antibodies gave identical staining in the hippocampus of wild-type (WT) mice. The specificity of the antibodies was demonstrated by the complete lack of signal in sections deriving form FAAH KO mice (C and D). Scale bar: 1 mm. Abbreviations: DG, dentate gyrus; hil., hilus; s.g., str. granulosum; s.m., str. moleculare; s.o., str. oriens; s.p., str. pyramidale; s.r., str. radiatum.

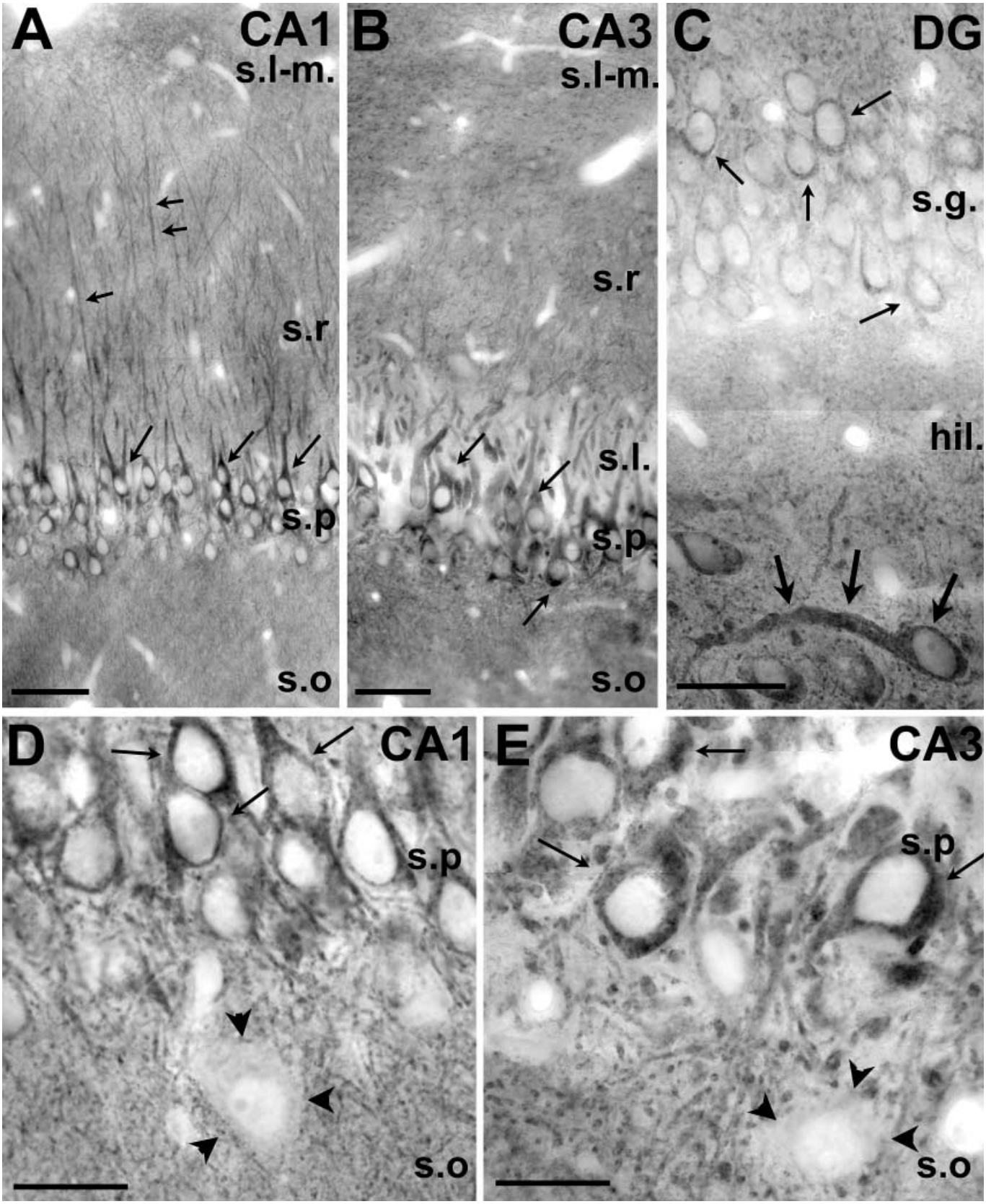

FIG. 2. FAAH is located in the principal cells of the hippocampus. (A–C) The somata and the dendrites (arrows) of the CA1 (A) and CA3 (B) pyramidal cells as well as the granule cells of the dentate gyrus (C) are immunopositive for FAAH. In the hilus of the dentate gyrus the mossy cells (large arrows) are also expressing FAAH. (D and E) Interneurons (arrowheads) can be identified as unstained elements in the FAAH-positive neuropil in str. oriens of the CA1 (D) and CA3 (E) areas. Some FAAH-positive pyramidal cell bodies are labelled with arrows. Scale bars, 100 μm (A and B); 50 μm (C); 20 μm (D and E). Abbreviations: DG, dentate gyrus; hil., hilus; s.g., str. granulosum; s.l., str. lucidum; s.l-m, str. lacunosum-moleculare; s.m., str. moleculare; s.o., str. oriens; s.p., str. pyramidale; s.r., str. radiatum.

the CA1 area. The only exception is that, due to the FAAH negativity of the numerous mossy fibres, the neuropil labelling is low in str. lucidum (Fig. 2B). In the gyrus dentatus, FAAH signal in the somata and dendrites of the granule cells is somewhat weaker than in the pyramidal cells. However, the staining is intense in the hilus. As shown in Fig. 2C, mossy cells express FAAH and the neuropil is also labelled. In contrast to the principal cells, interneurons do not show FAAH immunoreactivity. These cells can be identified as negative islands in the FAAH immunoreactive neuropil in all areas and layers (Fig. 2C and E).

To verify that FAAH is not present in inhibitory interneurons, we made double-immunofluorescent localization against FAAH and different neurochemical markers present in most (GAD65) or in smaller, functionally distinct subpopulations of interneurons (for

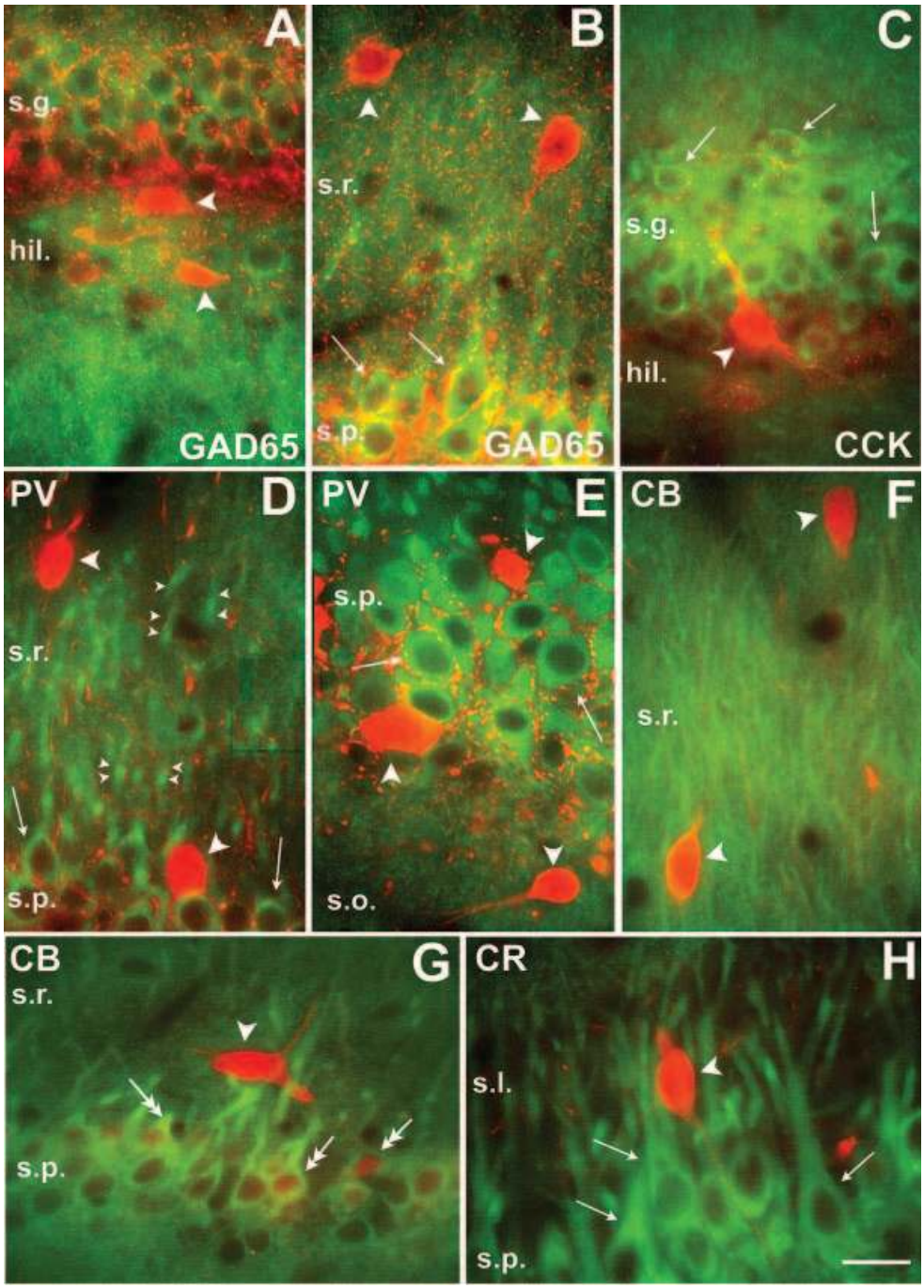

FIG. 3. FAAH is not detectable in GABAergic interneurons. Double-immunofluorescent staining against FAAH (green) and different markers (red) present in subpopulations of inhibitory interneurons. Arrowheads indicate interneurons negative for FAAH and positive for the given markers. FAAH-positive principal neurons are labelled with small arrows. Small arrowheads in D indicate FAAH-positive pyramidal cell dendrites in CA1 str. radiatum. In G, double arrowheads label CA1 pyramidal cells that are positive for both FAAH and calbindin D28k (CB). (A and C) Hilus of the dentate gyrus; (B, D, F and G) CA1 area; (E and H) CA3 area. The following GABAergic neuronal markers were examined: GAD65, glutamic acid decarboxylase 65 kDa; CCK, cholecystokinin; PV, parvalbumin; CB, calbindin D28k; CR, calretinin. Scale bars, 20 μm. Abbreviations: DG, dentate gyrus; hil., hilus; s.g., str. granulosum; s.l-m, str. lacunosum-moleculare; s.m., str. moleculare; s.o., str. oriens; s.p., str. pyramidale; s.r., str. radiatum.

review, see Freund & Buzsaki, 1996), such as CCK, PV, calbindin D28k (CB) and calretinin (CR). As shown in Fig. 3, none of the marker-containing inhibitory neurons expressed FAAH. Co-localization of two signals could only be seen in the case of CB labelling in the CA1 superficial pyramidal cells and the dentate granule cells, as these principal neurons express CB (Sloviter, 1989).

Ultrastructural localization of FAAH in the hippocampus

The electron microscopical localization of FAAH was studied both by immunoperoxidase (DAB, Fig. 4A) and by pre-embedding immunogold staining (Fig. 4B–D). The DAB precipitate filled the perinuclear cytoplasm, the dendrites and the dendritic spines of the principal cells in all areas. DAB reaction product was not present in mitochondria, but could often be seen enriched around smooth endoplasmic reticulum cisternae (Fig. 4A). In the hippocampus we never found FAAH-immunoreactive axon terminals. Immunogold staining, which allows high spatial resolution, localized FAAH primarily on the cytoplasmic surface of smooth endoplasmic reticulum cisternae and on the cytoplasmic surface of mitochondrial outer membranes. Gold signal could be detected only sparsely on the cytoplasmic side of the cell surface membranes. A quantitative analysis of the distribution of gold particles among different compartments, shown in Table 1, validates these conclusions. We did not observe labelling of glial processes either in the hippocampus or in the other examined brain regions at the electron microscopical level.

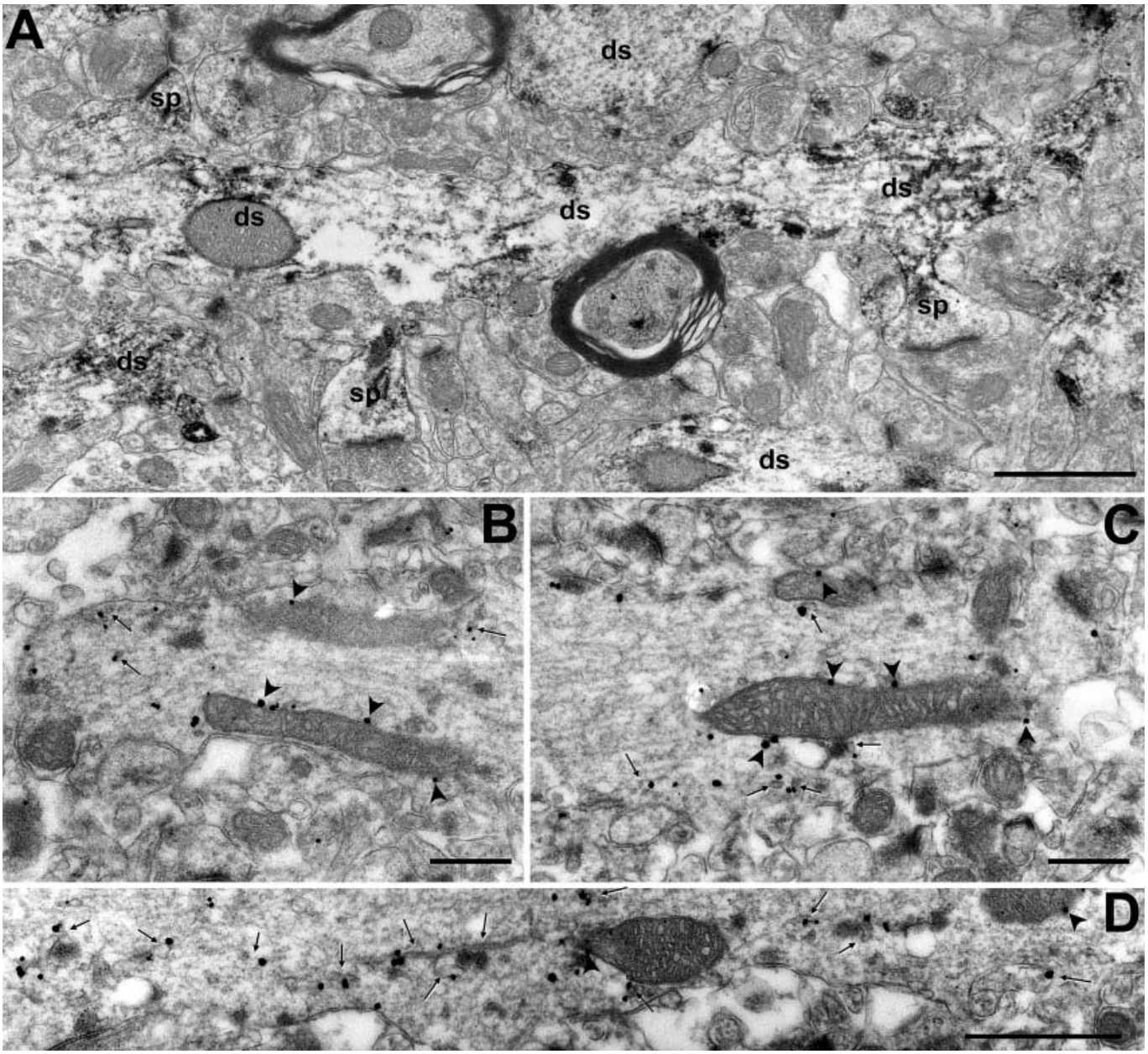

FIG. 4. Ultrastructural localization of FAAH in the hippocampus. FAAH immunoreactivity (diffuse DAB precipitate) is present in pyramidal cell secondary dendritic shafts (ds) and spines (sp) in CA3 str. oriens. While almost all shafts and spines are positive for FAAH in this figure, none of the axon terminals showed any immunoreactivity throughout the examined material. (B–D) Immunogold particles are primarily associated with parts of the endoplasmic reticulum (small arrows) and with the outer surface of the outer membranes of mitochondria (arrowheads). Labelling was less frequently detected in association with the plasma membrane. Scale bars, 1 μm (A); 0.5 μm (B and C); 0.2 μm (D).

TABLE 1. Distribution of FAAH immunogold labelling in the hippocampus

	Surface membrane	Smooth endoplasmic reticulum	Mitochondrial membrane	Cytoplasm	Total
Gold particles (*n*)	98	447	142	213	900
Distribution (%)	10.9	49.8	15.8	23.7	100

FAAH, fatty acid amide hydrolase.

Light and electron microscopical distribution of MGL in the hippocampus

A brief description of the findings at the light microscopical level was included in an earlier study (Dinh *et al*., 2002). Here we provide a more comprehensive description of these results complemented with electron microscopy.

A light microscopy examination of the immunostaining pattern for MGL (Fig. 5) suggests that this enzyme is associated with presynaptic axon terminals: principal cell bodies are negative for MGL. In the CA1 and CA3 areas the MGL-negative primary dendrites of the pyramidal cells can even be followed into the dendritic layers expressing a punctate neuropil staining. A dense, punctate, axon terminal-associated neuropil labelling is present in all other hippocampal layers, except the molecular layer of the dentate gyrus and the str. lacunosum-moleculare of the CA3 and CA1 areas. The dense MGL staining terminates abruptly at the CA1/subiculum border (Fig. 5D, broken line), suggesting that the signal derives from the presence of MGL in the axon terminals of CA3 pyramidal cells forming recurrent collaterals in the CA3 area and in the hilus as well as giving rise to the Schaffer collaterals in the CA1 subfield. The presence of large, MGL-positive varicosities in the CA3 str. lucidum (Fig. 5B and E, double arrowheads) suggests that axon terminals of granule cells, i.e. the mossy fibers, also express MGL.

Besides the dense punctate neuropil labelling, a more distinct, stronger signal is present in a subset of axon terminals in all hippocampal layers. Intensively stained varicosities can be found primarily around principal cell somata and resemble inhibitory cell terminals forming pericellular baskets (arrowheads on Fig. 5A–C). Pericellular baskets are also present around some of the hilar neurons (Fig. 5A, white arrowheads) that are otherwise negative for MGL. Labelled boutons can also be identified in association with thick, unstained principal cell primary dendrites in the CA1 and CA3 areas (Fig. 5C, double arrowheads). Occasionally, neuronal somata with features of interneurons are visualized by the staining (Fig. 5C). In these neurons the signal fills the endoplasmic reticulum in the cell body and proximal dendrites.

Our prediction from light microscopy, i.e. that MGL is present primarily in principal cell axon terminals, was unequivocally demonstrated at the electron microscopical level. Figure 6 shows that, in the CA1 area, axon terminals forming asymmetrical synapses with heads of pyramidal cell spines contain MGL. The DAB reaction end-product homogeneously filled vesicle-containing axon terminals, without any evident compartmental restriction. MGL-positive axon terminals forming asymmetrical synapses could also be found on inhibitory cell dendrites in all hippocampal layers. The presence of MGL in the axons of dentate granule cells has also been documented by electron microscopy. As shown in Fig. 7C, mossy fibres that contact the thorny excrescences of CA3 pyramidal cells in str. lucidum were densely filled with DAB reaction end-product. As in the case of FAAH we could find no MGL labelling in glial processes in none of the examined brain areas.

The light microscopical finding that the neuropil staining for MGL stopped abruptly at the CA1/subiculum border suggested that Schaffer collaterals, but not CA1 pyramidal cells axons, contain this enzyme. We further tested this possibility by a careful electron microscopic examination of asymmetrical synaptic inputs to horizontal interneuron dendrites in CA1 str. oriens. A subset of these interneurons was shown earlier to receive glutamatergic inputs mostly if not exclusively from local CA1 pyramidal cells (Blasco-Ibanez & Freund, 1995). Indeed, we found several dendrites of this type, which received asymmetrical synapses largely from MGL-negative boutons (Fig. 6D). Thus, CA1 pyramidal cell axons appear to lack MGL immunoreactivity.

The presence of MGL in subsets of inhibitory axon terminals, identified as the stained puncta in all layers of the CA1 area at the light microscopical level, has also been confirmed. Figure 7A and B demonstrates that MGL-positive terminals can be found both on somata (Fig. 7A) and axon initial segments (Fig. 7B) of principal cells. However, as shown in Fig. 7A, not all perisomatic inhibitory terminals are MGL-positive. Two subpopulations of perisomatically terminating inhibitory cell types have been described so far, containing either PV or CCK in their terminals (Acsady *et al*., 1996). CB_1 receptors were shown to be present only in the CCK-containing subset (Katona *et al*., 1999). In order to check whether the presence of MGL in perisomatic terminals correlates with the presence of these markers, we carried out double-immunostaining for both MGL and CCK. As shown in Fig. 8, in the case of perisomatic terminals the pre-embedding immunogold particles indicating the presence of CCK could always be found in terminals immunoreactive for MGL (labelled with diffuse DAB precipitation) in the CA3–CA1 areas. Thus, MGL is present in the CCK/CB_1-immunoreactive basket cell terminals. However, some PV-containing boutons are also likely to be immunoreactive for MGL, as CCK-negative/MGL-positive boutons were also found on the somata. In addition, chandelier cell axons innervating the axon initial segments of principal cells are known to contain PV, and they were also immunoreactive for MGL (Fig. 7B). It is important to note that, besides principal cells, inhibitory cell somata and dendrites were also innervated by MGL-containing inhibitory axons. Both MGL-negative and MGL-positive boutons forming symmetrical synapses have been found in the dendritic layers (Fig. 6B and C).

Distribution of FAAH and MGL in the amygdala

We found a significant difference in the intensity of FAAH-immunoreactivity between the basolateral and the central amygdala. While in the basolateral amygdala a strong cellular and neuropil staining was present outlining the structure, in the central amygdala the signal was very weak, represented by occasional neurons showing faint signal (Fig. 9). The texture of the labelling in the basolateral amygdala was similar to the hippocampus and cerebellum: the cytoplasm and the proximal dendrites, as well as the neuropil showed granular/reticular staining. It is important to note here that the regional distribution of FAAH matches the distribution of CB_1 receptors (see inset in Fig. 9A, photographed from the same material as Katona *et al*., 2001) in the examined amygdala nuclei.

Similarly to FAAH, the distribution of MGL also matched the presence or absence of CB_1 receptors in the basolateral and central amygdala (compare Figs 9 and 10). A punctate MGL staining was present in the basolateral amygdala, but was lacking in the central amygdala. Other amygdala nuclei showed only a background

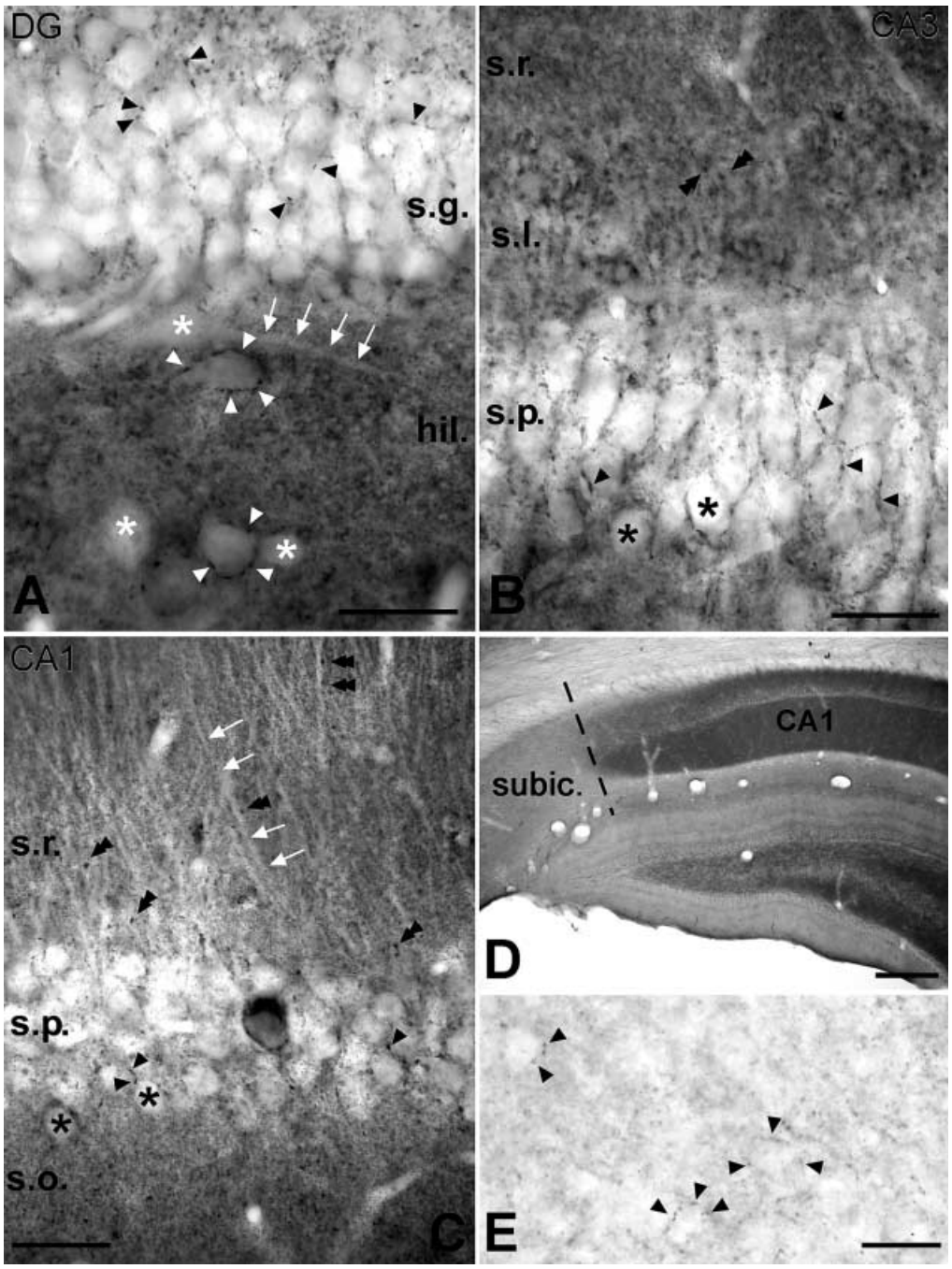

FIG. 5. Distribution of MGL in the hippocampus. The presence of a punctate signal in the neuropil and positive pericellular basket terminals characterizes MGL immunostaining. Principal cell bodies and dendrites remained negative indicating that MGL is likely located in axon terminals. (A) In the dentate gyrus (DG) pericellular baskets surround granule cells (black arrowheads) and some hilar neurons (white arrowheads). Note that some hilar neurons (asterisks) are not surrounded by MGL-positive terminals. On these cells the proximal dendrites (white arrows) are also devoid of MGL-positive terminals. (B) In the CA3 area, in addition to the neuropil labelling in str. radiatum and oriens, MGL-containing, pericellular baskets surround the pyramidal cells. In str lucidum, MGL staining visualizes the mossy terminals (double arrowheads). (C) In the CA1 subfield the neuropil labelling is similar to CA3. Here, pericellular baskets (arrowheads) in str. pyramidale and immunoreactive individual axon terminals in str. radiatum (double arrowheads) are also visible. The thick apical dendrites of pyramidal cells (white arrows) are negative for MGL. (D) The micrograph shows that MGL signal disappears at the CA1 area/subiculum border, i.e. where Schaffer collaterals end, suggesting that the neuropil staining in CA1–3 derives mostly from Schaffer collaterals. The axons of CA1 pyramidal cells projecting to the subiculum appear to lack MGL immunoreactivity. In str. lacunosum-moleculare and in the molecular layer of the dentate gyrus the signal is much weaker for MGL, suggesting that entorhinal afferents also lack this enzyme. (E) In the subiculum the neuropil labelling is considerably less dense than in CA1 str. radiatum. Most probably only axon terminals of inhibitory neurons are stained. They often surround unstained somata (arrowheads). Scale bars, 50 μm (A–C and E); 500 μm (D); Abbreviations: hil., hilus; s.g., str. granulosum; s.l., str. lucidum; s.o., str. oriens; s.p., str. pyramidale; s.r., str. radiatum; subic., subiculum.

level signal. Punctate staining was present in the neuropil and often surrounded somata. No signal could be seen in neuron cytoplasm.

The localization of the two enzymes at the ultrastructural level was studied in the basolateral amgdala using DAB as a chromogen for the immunoperoxidase reaction (Fig. 10C–F). Similarly to the hippocam-

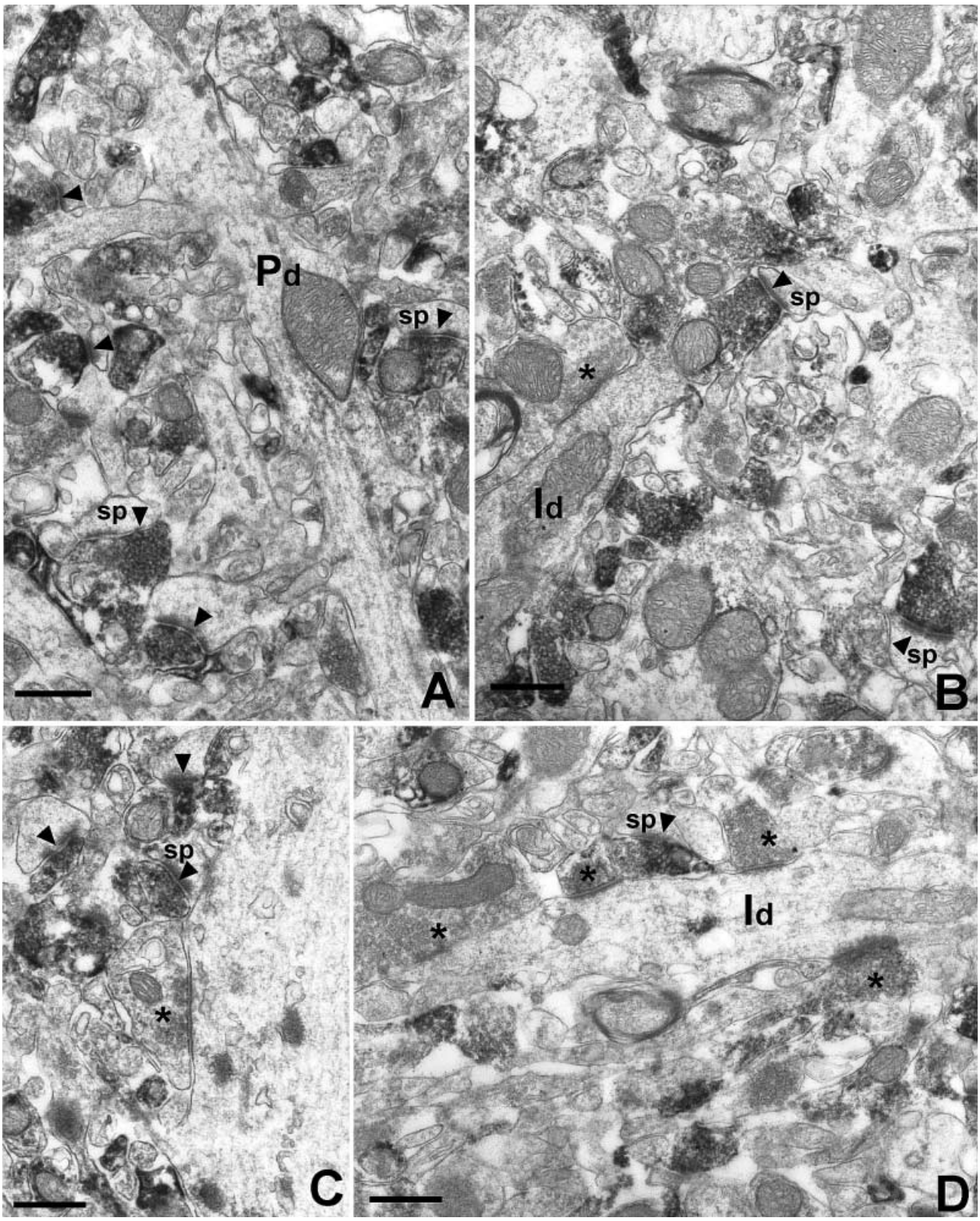

FIG. 6. Exclusive presynaptic localization of MGL in the hippocampus. (A) The spines (sp) of a second order pyramidal cell dendrite (Pd) in the CA1 region receive asymmetrical synapses from MGL-immunoreactive axon terminals (arrowheads). (B and C) Axon terminals forming symmetrical synapses (asterisks) on pyramidal cell (Pd in C) or interneuron (Id in B) dendrites are often negative for MGL, but positive examples are also common. Arrowheads label the positive terminals establishing asymmetrical contacts on spines. (D) The horizontally orientated inhibitory cell dendrite (Id) in str. oriens of the CA1 subfield is densely covered with MGL-negative axon terminals (asterisks) forming asymmetrical synapses. These boutons likely originate from local CA1 pyramidal cell collaterals that are known to account for the majority of synaptic input of these interneurons. A neighbouring dendritic spine is innervated by an MGL-positive axon terminal, probably of Schaffer collateral origin. Scale bars, 0.5 μm.

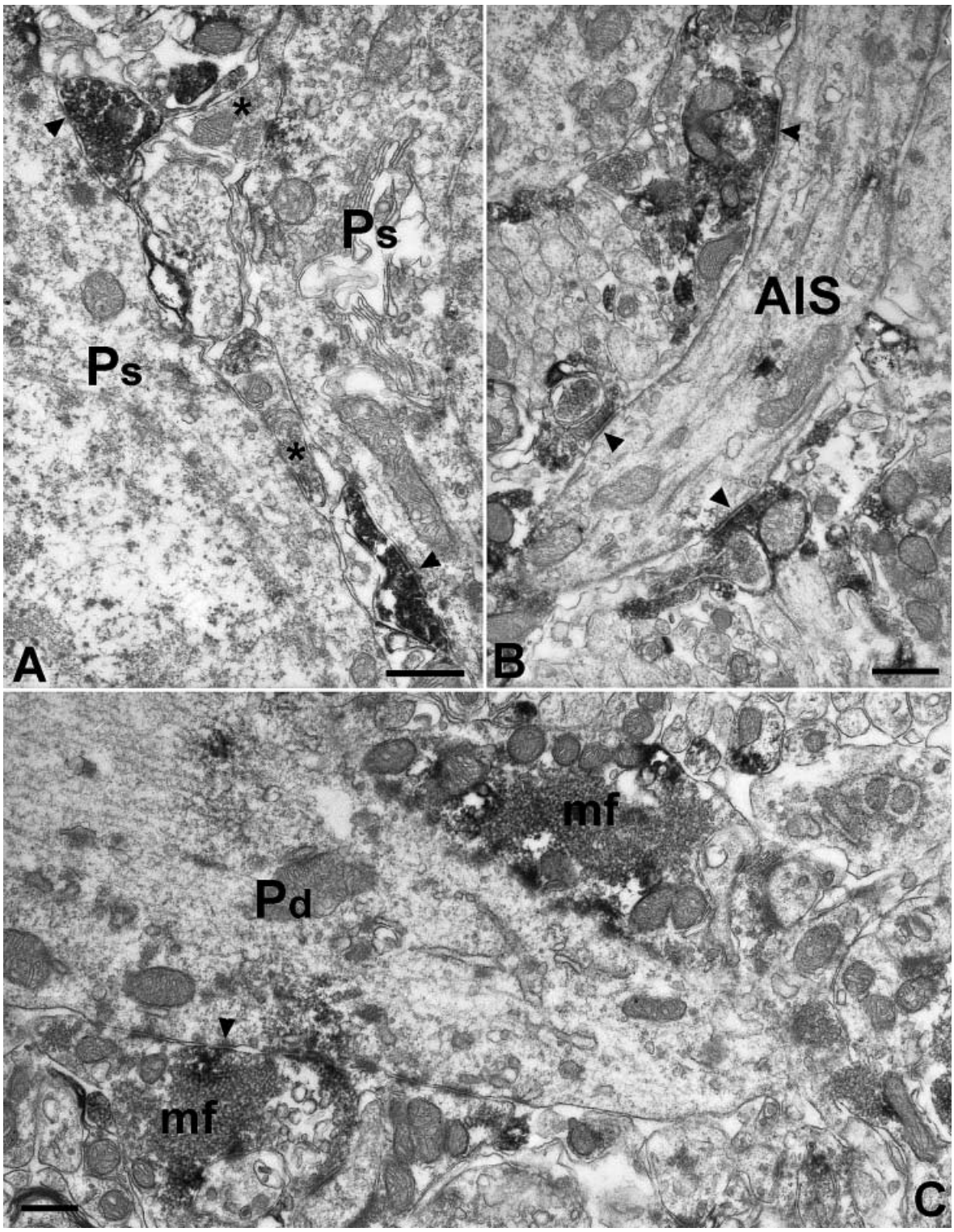

FIG. 7. The majority of perisomatic inhibitory axon terminals and the mossy terminals are immunoreactive for MGL. (A) MGL-positive basket cell terminals form symmetrical synapses (arrowheads) on the somata of pyramidal cells (Ps) in the CA1 area. Note that MGL-negative (asterisks) basket cell terminals are also present. (B) Axon terminals of chandelier cells forming symmetrical synapses (arrowheads) on pyramidal cell axon initial segments (AIS) are also positive for MGL. (C) Two mossy fibre terminals (mf) surround the thick proximal dendrite (Pd) of a pyramidal cell in CA3 str. lucidum. Scale bars, 0.5 μm.

pus, the distribution of the signal for the two proteins was complementary. FAAH was present in dendrites of different diameter and in somata. The DAB precipitate often accumulated in the vicinity of mitochondria (Fig. 10C and D). In contrast, MGL signal was seen in axon terminals loaded with vesicles and forming either symmetrical or asymmetrical synapses on MGL-negative dendritic profiles. This suggests that MGL is present in subsets of both excitatory and inhibitory terminals (Fig. 10E and F).

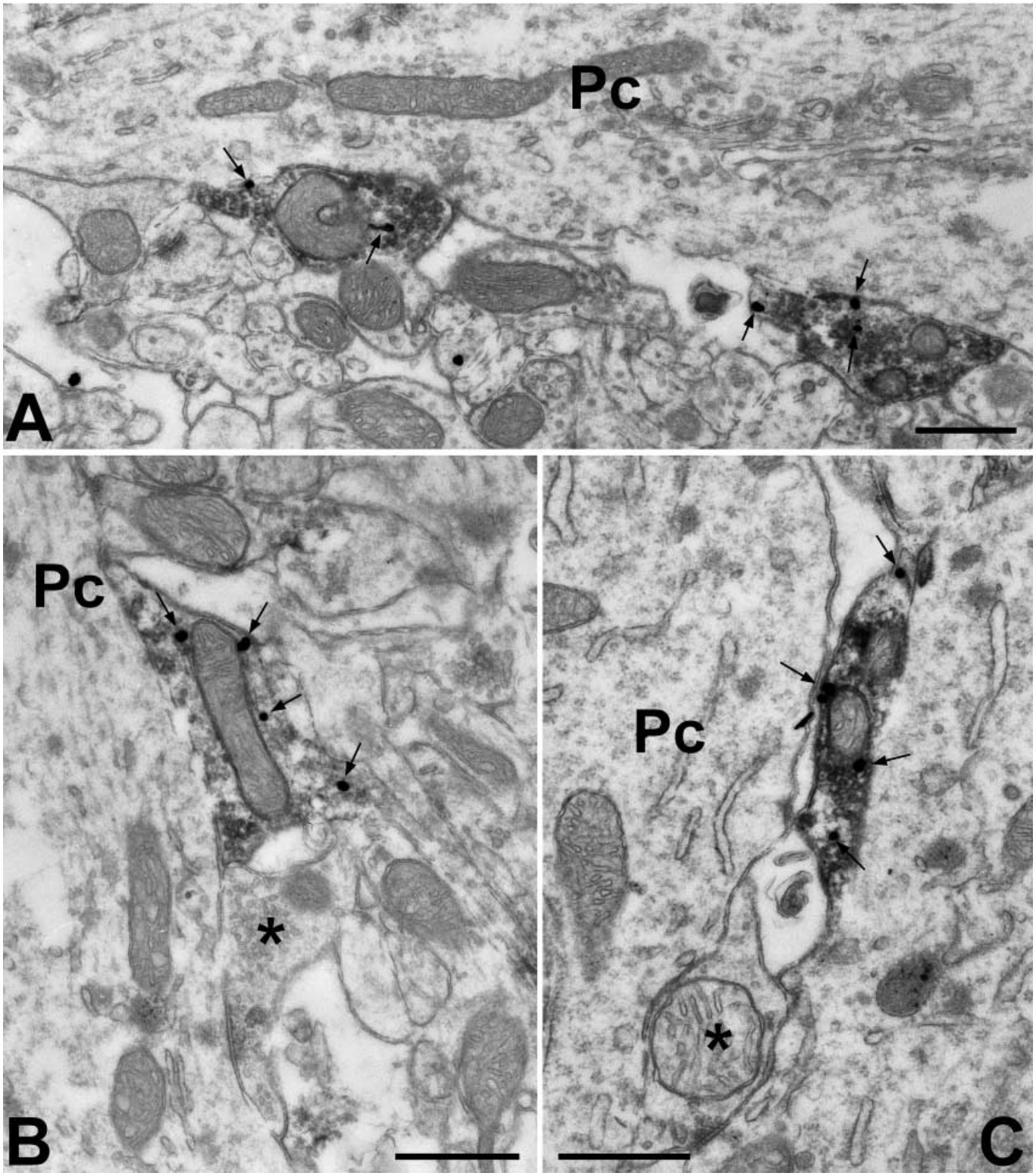

FIG. 8. MGL is present in CCK-containing basket cell terminals in the CA1–3 regions. MGL was visualized using immunoperoxidase reaction and DAB as a chromogen producing a diffuse electron-dense end-product, whereas CCK immunoreactivity is represented by silver-intensified immunogold particles (arrows). A large proportion of the MGL-positive boutons synapsing on pyramidal cell bodies (Pc) were also immunoreactive for CCK, but additional basket cell terminals (asterisks) negative for both antigens were also visible. These terminals most probably derive from PV-IR basket cells. Scale bars, 0.5 μm.

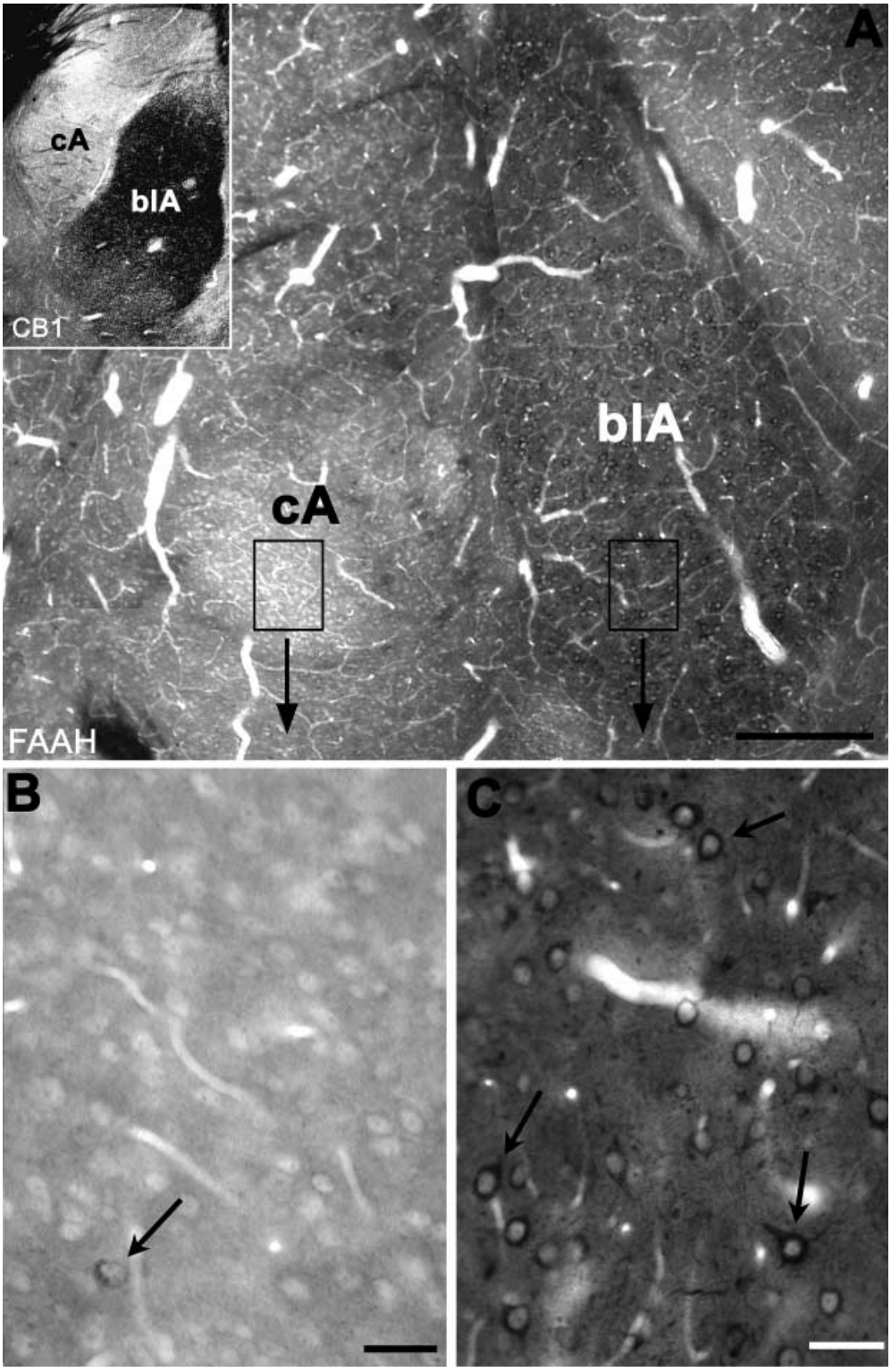

FIG. 9. Fatty acid amide hydrolase (FAAH) expression correlates with the presence of cannabinoid receptors subtype 1 (CB_1) receptor immunoreactivity in divisions of the amygdala. (A) Neurons of the basolateral amygdala (blA) are heavily immunoreactive for FAAH in contrast to the central amygdala (cA), where hardly any cells contain this enzyme. The inset shows the correlation with the relative distribution of CB_1 receptor in the different nuclei. The boxed areas in A are shown at higher magnification in B and C. (B) Occasional neuronal staining (arrow) and the lack of neuropil immunoreactivity has been observed in the central amygdala. (C) Intensively labelled cell bodies (arrows) and primary dendrites are visualized by FAAH immunoreactivity in addition to the immunostained neuropil in the basolateral amygdala. The same region expresses strong CB_1 receptor immunoreactivity, although this staining is known to be confined to axons (see Katona *et al*., 2001). Scale bars, 250 μm (A); 50 μm (B and C).

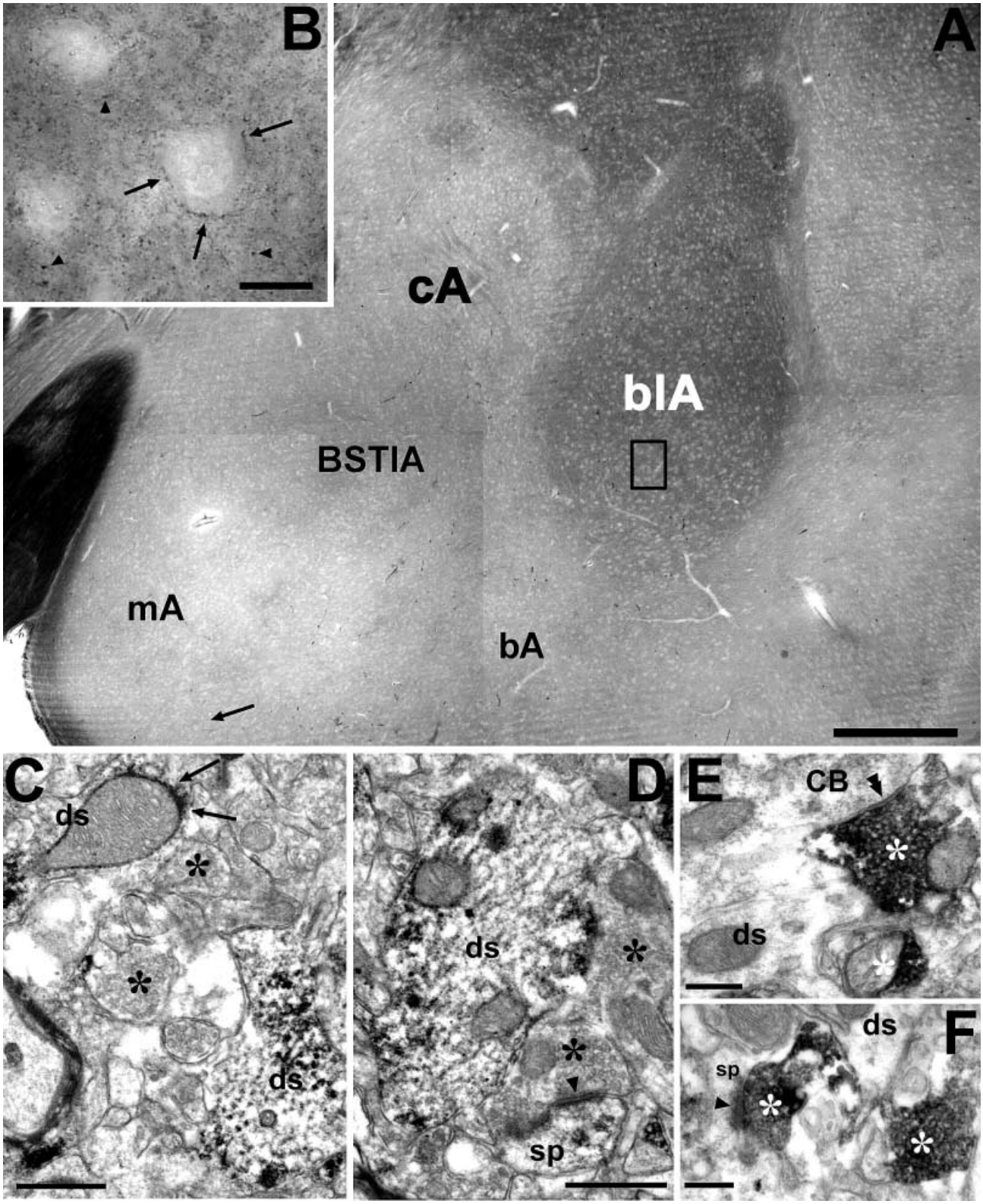

FIG. 10. Ultrastructural segregation of MGL and FAAH in the amygdala. (A) While there is a dense neuropil signal in the basolateral amygdala (blA), the central amygdala (cA) shows weak immunoreactivity. Nearby structures express low levels of MGL [bed nucleus of the stria terminalis-intra-amygdaloid division (BSTIA)] or no MGL at all [medial amygdala nuclei (mA)]. (B) Enlarged view of the boxed area in A. The neuropil staining derives from immunoreactive puncta, possibly axon terminals some of which form pericellular baskets (arrows) or are present in the neuropil (arrowheads). (C and D) FAAH immunostaining is present postsynaptically in the amygdala, in dendritic shafts (ds) and spines (sp.). (C) Arrows indicate that in larger dendrites the DAB end-product is accumulated around mitochondria. Asterisks label FAAH-negative axon terminals. One of them forms an asymmetrical synapse (arrowhead) on a labelled spine head. (E and F) MGL immunostaining is present presynaptically in subsets of axon terminals (white asterisks). (E) A putative inhibitory terminal, as it forms a symmetrical synapse (double arrowhead) on a cell body. The left terminal on (F) forms an asymmetrical synapse on a dendritic spine, identifying it as an excitatory terminal. Scale bars, 500 μm (A); 10 μm (B); 0.5 μm (C and D); 0.2 μm (E and F).

Light and electron microscopic distribution of FAAH in the cerebellum

In contrast to the finding of Egertova *et al*. (2003), we found that not only the somata, but the entire dendritic arbor of Purkinje cells expressed high levels of FAAH immunoreactivity, resulting in a layer-selective labelling in the cerebellum (Fig. 11). Similar to the hippocampus, the immunostaining showed a granular-reticular pattern that was especially evident in the cytoplasm of the large Purkinje cells. In the granule cell layer occasional axon terminals proved to be FAAH-positive, primarily at the border of the Purkinje cell/granule cell layers. These axon terminals were large and often surrounded FAAH-negative, small, horizontally elongated cell bodies in the Purkinje cell layer (inset in Fig. 11). Granule cells showed faint signal, close to the threshold of immunocytochemical detection. We also examined the immunostaining of different interneuron types located in various cerebellar layers, i.e. Golgi, basket and stellate cells (Fig. 11C and D). Here the staining intensity was similar to the signal in the granule cells; thus,

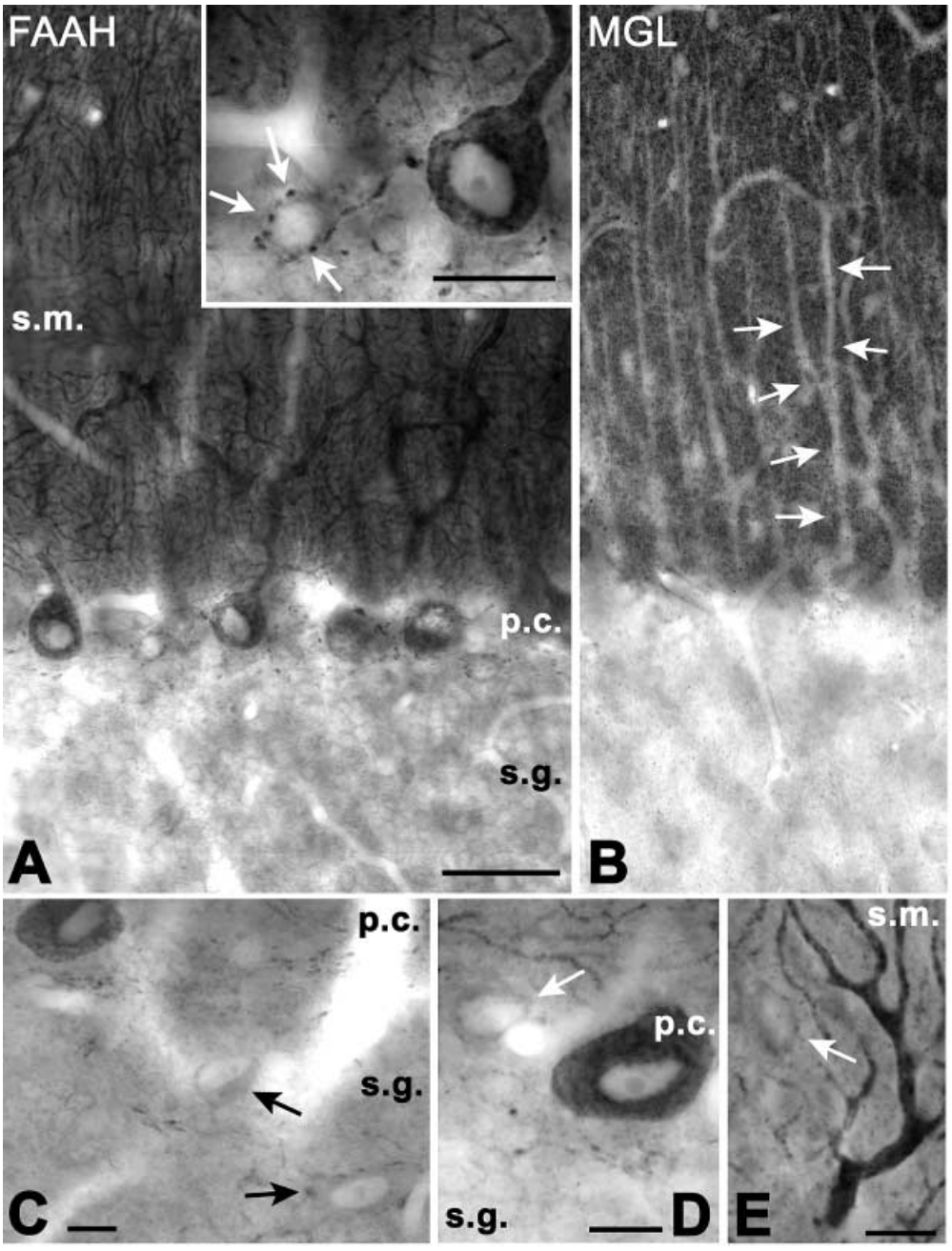

FIG. 11. Complementary distribution of fatty acid amide hydrolase (FAAH) and monoglyceride lipase (MGL) in str. moleculare of the cerebellum. (A) Purkinje cell bodies and their entire dendritic arbor is strongly immunostained for FAAH in the molecular (s.m.) and Purkinje cell (p.c.) layers, in contrast to the occasional axonal labelling (arrows in inset) surrounding small FAAH-negative cell bodies just below the Purkinje cell layer. (B) The MGL-negative Purkinje cell dendrites (arrows) stand out from the darkly immunoreactive neuropil that likely consists of MGL-positive axon terminals. (C–E) Interneurons (arrows) in the granule (C) and Purkinje cell layer (D), as well as in the molecular layer (E) showed weak if any immunoreactivity, close to the immunocytochemical detection threshold. Scale bars, 40 μm (A); 20 μm (B); 10 μm (C–E). Abbreviations: p.c., Purkinje cell layer; s.g., str. granulosum; s.m., str. moleculare.

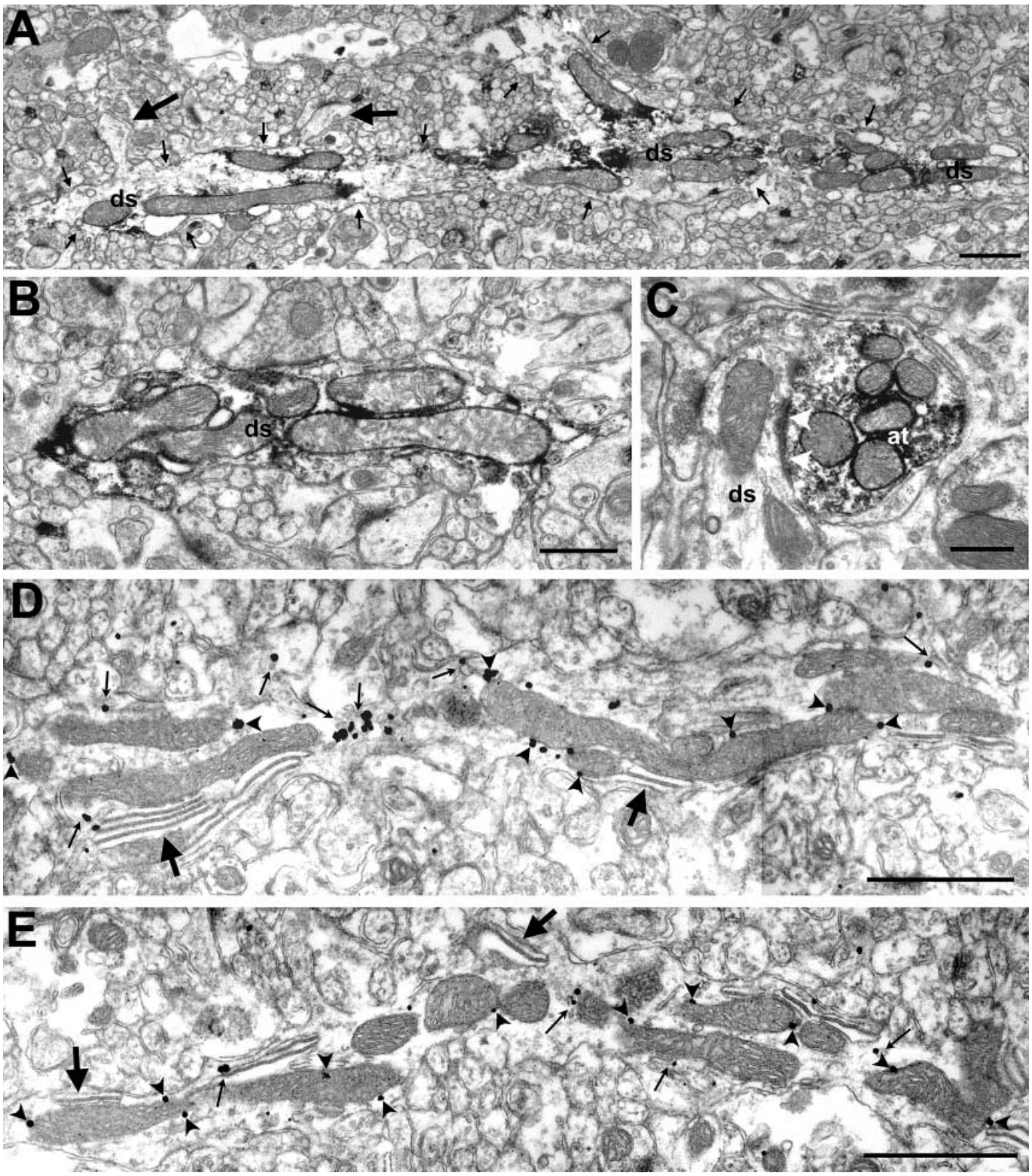

FIG. 12. Ultrastructural localization of FAAH in the cerebellum. Immunoperoxidase reaction using DAB as a chromogen visualized Purkinje cell dendrites (ds) and spines (large arrows) in the molecular layer (A and B) and a few axon terminals (C) at the border of the Purkinje and granule cell layers. The presence of dendritic spines (large arrows) identifies the branching dendrite (outlined by small arrows) as belonging to a Purkinje cell in A. (C) A FAAH-positive axon terminal (at) forms a synapse (white arrowheads) on a FAAH-negative dendrite (ds) in stratum granulosum. (D and E) Immunogold particles indicate that FAAH is associated with membranes, as expected from a protein with transmembrane domains. It is primarily located on the outer surface of the outer membranes of mitochondria (arrowheads) and on the surface of the endoplasmic reticulum (small arrows). The plasma membrane and the stacked cisternae of the smooth endoplasmic reticulum (large arrows) rarely showed any labelling for FAAH. Scale bars, 1 μm (A, D and E); 0.5 μm (B, C).

TABLE 2. Distribution of FAAH immunogold labelling in the cerebellum

	Surface membrane	Smooth endoplasmic reticulum	Stacked lamellae of endoplasmic reticulum	Mitochondrial membrane	Cytoplasm	Total
Gold particles (*n*)	9	265	11	210	67	562
Distribution (%)	1.6	47.2	2.0	37.4	11.9	100

FAAH, fatty acid amide hydrolase.

compared to the Purkinje cells, the inhibitory interneurons can be considered FAAH-negative.

The electron microscopic examination confirmed our light microscopic finding that in the molecular and Purkinje cell layers only the dendrites of the Purkinje cells express FAAH (Fig. 12A, B, D and E). Immunoreactivity was present in the thick primary and the thinner higher order dendrites of the Purkinje cells. The signal in the spines was not as evident as in hippocampal pyramidal cells. The presence of FAAH in the granule cell layer axons was also confirmed at the electron microscopic level (Fig. 12C). The labelled axon terminals formed synapses on FAAH-negative somata and dendrites.

The immunogold signal, similar to the hippocampus, was located primarily on the cytoplasmic surface of the mitochondrial outer membranes and on the cytoplasmic surface of smooth endoplasmic reticulum cisternae. The surface membranes and the stacked cisternae of the smooth endoplasmic reticulum were mostly devoid of FAAH (Fig. 12D and E). The quantitative results on the distribution of the gold particles, shown in Table 2, demonstrate that the overall picture is similar to the hippocampus. The difference observed arose from the higher incidence of gold particles over mitochondrial membranes at the expense of labelling over the surface membrane and the cytoplasm.

Light microscopical distribution of MGL in the cerebellum

Similarly to the hippocampus, the localization of MGL and FAAH is also complementary in the cerebellum. This can be clearly seen in Fig. 11. In Fig. 11B, the negative Purkinje cell dendrites stand out from a background of MGL-positive puncta in str. moleculare, making it possible to follow even the second order thinner dendrites of the cells. A considerably less dense punctate staining was present in str. granulosum. Clusters of immunolabelled puncta outlined small, MGL-negative patches that correspond to glomeruli. Thus, these puncta are likely to be Golgi cell terminals.

Discussion

The major finding of our study is that FAAH is localized in the soma-dendritic compartment, whereas MGL is localized in axons. Furthermore, our results also allow various conclusions to be made. First, in the hippocampus, FAAH is present postsynaptically in somata and dendrites of principal neurons, but is absent from inhibitory interneurons. Second, in the cerebellum, Purkinje cell somata and dendrites, as well as a small subpopulation of axon terminals express FAAH. Third, in the hippocampus and cerebellum FAAH is located primarily on the cytosolic surface of smooth endoplasmic reticulum cisternae and mitochondrial outer membranes, with only a very small proportion of the enzyme associated with cell membranes. Fourth, the distribution of MGL parallels that of CB_1 receptors and FAAH at the regional level, whereas it is complementary to FAAH distribution at the ultrastructural level. Fifth, in the hippocampus MGL is present in axon terminals of granule cells and CA3 pyramidal cells throughout their entire axonal arborization. A subpopulation of inhibitory axon terminals, including those of CCK-immunoreactive basket cells and axo-axonic cells, also express MGL. Sixth, in the cerebellum MGL immunostaining is present only in str. moleculare in the form of punctate axonal labelling. Seventh, in the amygdala FAAH and MGL expression matches that of the CB_1 receptors, i.e. they are present in the basolateral nucleus, but are nearly absent from the central nucleus. Eighth, the ultrastructural distribution of the two materials in the amygdala, similar to the hippocampus, is complementary: i.e. FAAH is located postsynaptically, MGL presynaptically.

FAAH is associated with intracellular membranes of principal neurons

We confirmed earlier results (Egertova *et al*., 1998; Tsou *et al*., 1998b) suggesting that the distributions of CB_1 and FAAH, while overlapping in several regions of the brain, are complementary at the cellular level. In the hippocampus and cerebellum, CB1 receptors are located presynaptically on axon terminals of subsets of inhibitory neurons (Tsou *et al*., 1998a; Katona *et al*., 1999) and in the cerebellum probably also on excitatory axons, whereas FAAH is found in dendrites of postsynaptic principal neurons. As expected from its structure, FAAH may be located on the cytoplasmic surface of membranes. However, quite unexpectedly, the enzyme was primarily associated with intracellular membranes, including smooth endoplasmic reticulum cisternae and the external surface of the mitochondria, but not with the plasma membrane.

X-ray crystallography studies suggest that anandamide may access the active site of FAAH from the lipid membrane (Bracey *et al*., 2002). During the breakdown phase of endocannabinoids fatty acid amides can be internalized by endocytosis into lipid vesicles that later fuse with endoplasmic reticulum and mitochondria membranes, where FAAH would degrade these lipids. Alternatively, anandamide must cross the cell membrane and travel through the cytosol to the endoplasmic reticulum. The first step may involve a transmembrane transport system (Beltramo *et al*., 1997; Hillard *et al*., 1997), which remains to be molecularly characterized, while the second might implicate one or more intracellular lipid-binding protein(s). It is important to point out that, in addition to anandamide, FAAH is responsible for the hydrolysis of other fatty acid amides with potent biological actions. These include the endogenous ligand for peroxisome-proliferator-activated receptors, oleoylethanolamide (Rodriguez de Fonseca *et al*., 2001; Fu *et al*., 2003), and the anti-inflammatory/analgesic mediator palmitoylethanolamide (Mazzari *et al*., 1996; Calignano *et al*., 2000). Although 2-AG is hydrolysed by FAAH in broken cell preparations (Goparaju *et al*., 1998), FAAH −/− mice have normal brain 2-AG levels (Lichtman *et al*., 2002), indicating that FAAH does not contribute to 2-AG degradation *in vivo*. Our results, showing that FAAH and MGL are preferentially localized in distinct neuronal compartments, provide a possible explanation for this discrepancy.

The lack of FAAH in GABAergic interneurons is going to provide good guidance in the identification of the precise function(s) of FAAH. For example, the presence or lack of depolarization-induced suppression of inhibition, and the associated endocannabinoid release, may shed light on the involvement of FAAH in this phenomenon.

MGL is located presynaptically in axons of subsets of excitatory and inhibitory neurons

The distribution of MGL immunoreactivity in the hippocampus and amygdala suggests that this endocannabinoid-degrading enzyme has a selective presynaptic localization. It can be found in the axons of dentate granule cells and CA3 pyramidal cells, i.e. in the mossy fibre terminals and in the Schaffer collaterals. MGL is present presynaptically in the cerebellum as well as in the molecular layer where parallel and climbing fibres terminate. In the hippocampus, cannabimimetic agents reduce glutamatergic EPSCs in CB_1 –/– mice (Hajos *et al*., 2001), suggesting that glutamatergic axon terminals express a novel cannabinoid-sensitive receptor. In the cerebellum, depolarization-induced suppression of excitation has been demonstrated on parallel and climbing fibres terminating on Purkinje cells (Kreitzer & Regehr, 2001b), but similar effects in the hippocampus could only be evoked in a single study using very long depolarizing pulses (Ohno-Shosaku *et al*., 2002). The effect could be modulated by cannabinoid antagonists and agonists, and was absent in CB_1 KO mice. Thus, the release of glutamate from excitatory terminals might be under the control of endocannabinoids in both regions. The presence of MGL in glutamatergic fibres might be necessary to terminate the effect of endocannabinoids on excitatory transmission. The fact that MGL is not present in str. lacunosum-moleculare, neither in the dentate molecular layer nor in the subiculum, suggests that inputs from the entorhinal cortex and from the CA1 area are not controlled by endocannabinoids. This prediction has yet to be tested, as no data are available on the existence of depolarization-induced suppression of excitation or the modulation of glutamate release in the perforant pathway or the subiculum.

Besides excitatory terminals, subsets of hippocampal and amygdala interneurons express MGL in their axon terminals. Two populations of axon terminals proved to contain MGL. The presence of MGL in the CCK-positive subpopulation of interneurons can be explained by the fact that these cells also express CB_1 receptors (Katona *et al*., 1999). Thus, similarly to glutamatergic terminals, MGL might terminate the effect of endocannabinoids in this population of axon terminals. The presence of MGL in the axo-axonic cell terminals needs an alternative explanation, as these inhibitory axons do not express CB_1 receptors. In the granule cell layer of the cerebellum we observed a punctate terminal labelling surrounding negative areas with the size of glomeruli formed by granule cell dendrites, mossy fibres and Golgi cell axon terminals. Because the inhibitory terminals of Golgi cells are located on the periphery of the glomeruli (Hamori & Takacs, 1989), the observed punctate signal among the granule cells most probably derives from the Golgi cell terminals and preterminal axons. Thus, it seems that at least one subpopulation of cerebellar inhibitory cells expresses FAAH in their axons.

Because the ultrastructural localization of synthesis, mechanism of release, site and speed of transport of endocannabinoids are not yet known, the functional implications of these findings are limited at present. We can only speculate as to why the two enzymes of endocannabinoid hydrolysis are located in complementary compartments. Based on available evidence, we suggest that FAAH may set the resting level of anandamide close to its sites of synthesis, while MGL may help to inactivate 2-AG close to its sites of action. This hypothesis is in agreement with the cellular localization of FAAH in proximity of Ca^{2+} stores (mitochondria, endoplasmic reticulum), where Ca^{2+}-dependent anandamide synthesis might take place. However, to fully understand the cycle of endocannabinoids synthesis, release and deactivation, it will be necessary to characterize all components of this cycle, including synthetic enzymes and transporters, and provide a detailed description of their localization and kinetics of actions.

Acknowledgements

We are grateful to Dr I. Katona for valuable contributions at preliminary stages of the study, to Dr N. Hájos for helpful discussions, and to Mrs K. Lengyel, Ms E. Simon, Ms K. Ivanyi and Mr Gy. Goda for the excellent technical assistance. This work was supported by the Howard Hughes Medical Institute (USA), NIH (MH 54 671, NS30549, DA13173, DA15197, DA-12493 and DA-12447), Philip Morris External Research Program and OTKA (T034638 and T032251, Hungary). F.B. was supported by the University of Naples 'Federico II', School of Medicine PhD program.

Abbreviations

2-AG, sn-2-arachidonoyl-glycerol; CB_1, cannabinoid receptors subtype 1; CCK, cholecystokinin; DAB, diaminobenzidine; FAAH, fatty acid amide hydrolase; GABA, γ-aminobutyric acid; MGL, monoglyceride lipase; PB, phosphate buffer; PV, parvalbumin.

References

Acsady, L., Gorcs, T.J. & Freund, T.F. (1996) Different populations of vasoactive intestinal polypeptide-immunoreactive interneurons are specialized to control pyramidal cells or interneurons in the hippocampus. *Neuroscience*, **73**, 317–334.

Beltramo, M., Stella, N., Calignano, A., Lin, S.Y., Makriyannis, A. & Piomelli, D. (1997) Functional role of high-affinity anandamide transport, as revealed by selective inhibition. *Science*, **277**, 1094–1097.

Blasco-Ibanez, J.M. & Freund, T.F. (1995) Synaptic input of horizontal interneurons in stratum oriens of the hippocampal CA1 subfield: structural basis of feed-back activation. *Eur. J. Neurosci.*, **7**, 2170–2180.

Bracey, M.H., Hanson, M.A., Masuda, K.R., Stevens, R.C. & Cravatt, B.F. (2002) Structural adaptations in a membrane enzyme that terminates endocannabinoid signaling. *Science*, **298**, 1793–1796.

Cadas, H., di Tomaso, E. & Piomelli, D. (1997) Occurrence and biosynthesis of endogenous cannabinoid precursor, N-arachidonoyl phosphatidylethanolamine, in rat brain. *J. Neurosci.*, **17**, 1226–1242.

Calignano, A., La Rana, G., Loubet-Lescoulie, P. & Piomelli, D. (2000) A role for the endogenous cannabinoid system in the peripheral control of pain initiation. *Prog. Brain Res.*, **129**, 471–482.

Cravatt, B.F., Demarest, K., Patricelli, M.P., Bracey, M.H., Giang, D.K., Martin, B.R. & Lichtman, A.H. (2001) Supersensitivity to anandamide and enhanced endogenous cannabinoid signaling in mice lacking fatty acid amide hydrolase. *Proc. Natl Acad. Sci. USA*, **98**, 9371–9376.

Devane, W.A., Dysarz, F.A. 3rd, Johnson, M.R., Melvin, L.S. & Howlett, A.C. (1988) Determination and characterization of a cannabinoid receptor in rat brain. *Mol. Pharmacol.*, **34**, 605–613.

Devane, W.A., Hanus, L., Breuer, A., Pertwee, R.G., Stevenson, L.A., Griffin, G., Gibson, D., Mandelbaum, A., Etinger, A. & Mechoulam, R. (1992) Isolation and structure of a brain constituent that binds to the cannabinoid receptor. *Science*, **258**, 1946–1949.

Dinh, T.P., Carpenter, D., Leslie, F.M., Freund, T.F., Katona, I., Sensi, S.L., Kathuria, S. & Piomelli, D. (2002) Brain monoglyceride lipase participating in endocannabinoid inactivation. *Proc. Natl Acad. Sci. USA*, **99**, 10819–10824.

Egertova, M., Cravatt, B.F. & Elphick, M.R. (2003) Comparative analysis of fatty acid amide hydrolase and cb(1) cannabinoid receptor expression in the mouse brain: evidence of a widespread role for fatty acid amide hydrolase in regulation of endocannabinoid signaling. *Neuroscience*, **119**, 481–496.

Egertova, M., Giang, D.K., Cravatt, B.F. & Elphick, M.R. (1998) A new perspective on cannabinoid signalling: complementary localization of fatty acid amide hydrolase and the CB1 receptor in rat brain. *Proc. R. Soc. Lond. B Biol. Sci.*, **265**, 2081–2085.

Freund, T.F. & Buzsaki, G. (1996) Interneurons of the hippocampus. *Hippocampus*, **6**, 345–470.

Fu, J., Gaetani, S., Oveisi, F., Lo Verme, J., Serrano, A., Rodriguez de Fonseca, F., Rosengarth, A., Luecke, H., Di Giacomo, B., Tarzia, G. & Piomelli, D. (2003) Oleylethanolamide regulates feeding and body weight through activation of the nuclear receptor PPAR-alpha. *Nature*, **425**, 90–93.

Goparaju, S.K., Ueda, N., Yamaguchi, H. & Yamamoto, S. (1998) Anandamide amidohydrolase reacting with 2-arachidonoylglycerol, another cannabinoid receptor ligand. *FEBS Lett.*, **422**, 69–73.

Hajos, N., Katona, I., Naiem, S.S., MacKie, K., Ledent, C., Mody, I. & Freund, T.F. (2000) Cannabinoids inhibit hippocampal GABAergic transmission and network oscillations. *Eur. J. Neurosci.*, **12**, 3239–3249.

Hajos, N., Ledent, C. & Freund, T.F. (2001) Novel cannabinoid-sensitive receptor mediates inhibition of glutamatergic synaptic transmission in the hippocampus. *Neuroscience*, **106**, 1–4.

Hamori, J. & Takacs, J. (1989) Two types of GABA-containing axon terminals in cerebellar glomeruli of cat: an immunogold-EM study. *Exp. Brain Res.*, **74**, 471–479.

Herkenham, M., Lynn, A.B., Little, M.D., Johnson, M.R., Melvin, L.S., de Costa, B.R. & Rice, K.C. (1990) Cannabinoid receptor localization in brain. *Proc. Natl Acad. Sci. USA*, **87**, 1932–1936.

Hillard, C.J., Edgemond, W.S., Jarrahian, A. & Campbell, W.B. (1997) Accumulation of N-arachidonoylethanolamine (anandamide) into cerebellar granule cells occurs via facilitated diffusion. *J. Neurochem.*, **69**, 631–638.

Hoffman, A.F. & Lupica, C.R. (2000) Mechanisms of cannabinoid inhibition of GABA(A) synaptic transmission in the hippocampus. *J. Neurosci.*, **20**, 2470–2479.

Katona, I., Rancz, E.A., Acsady, L., Ledent, C., Mackie, K., Hajos, N. & Freund, T.F. (2001) Distribution of CB1 cannabinoid receptors in the amygdala and their role in the control of GABAergic transmission. *J. Neurosci.*, **21**, 9506–9518.

Katona, I., Sperlagh, B., Sik, A., Kafalvi, A., Vizi, E.S., Mackie, K. & Freund, T.F. (1999) Presynaptically located CB1 cannabinoid receptors regulate GABA release from axon terminals of specific hippocampal interneurons. *J. Neurosci.*, **19**, 4544–4558.

Kreitzer, A.C. & Regehr, W.G. (2001a) Cerebellar depolarization-induced suppression of inhibition is mediated by endogenous cannabinoids. *J. Neurosci.*, **21**, RC174.

Kreitzer, A.C. & Regehr, W.G. (2001b) Retrograde inhibition of presynaptic calcium influx by endogenous cannabinoids at excitatory synapses onto Purkinje cells. *Neuron*, **29**, 717–727.

Lichtman, A.H., Hawkins, E.G., Griffin, G. & Cravatt, B.F. (2002) Pharmacological activity of fatty acid amides is regulated, but not mediated, by fatty acid amide hydrolase in vivo. *J. Pharmacol. Exp. Ther.*, **302**, 73–79.

Mailleux, P. & Vanderhaeghen, J.J. (1992) Distribution of neuronal cannabinoid receptor in the adult rat brain: a comparative receptor binding radioautography and in situ hybridization histochemistry. *Neuroscience*, **48**, 655–668.

Matsuda, L.A., Lolait, S.J., Brownstein, M.J., Young, A.C. & Bonner, T.I. (1990) Structure of a cannabinoid receptor and functional expression of the cloned cDNA. *Nature*, **346**, 561–564.

Mazzari, S., Canella, R., Petrelli, L., Marcolongo, G. & Leon, A. (1996) N-(2-hydroxyethyl) hexadecanamide is orally active in reducing edema formation and inflammatory hyperalgesia by down-modulating mast cell activation. *Eur. J. Pharmacol.*, **300**, 227–236.

Misner, D.L. & Sullivan, J.M. (1999) Mechanism of cannabinoid effects on long-term potentiation and depression in hippocampal CA1 neurons. *J. Neurosci.*, **19**, 6795–6805.

Ohno-Shosaku, T., Maejima, T. & Kano, M. (2001) Endogenous cannabinoids mediate retrograde signals from depolarized postsynaptic neurons to presynaptic terminals. *Neuron*, **29**, 729–738.

Ohno-Shosaku, T., Tsubokawa, H., Mizushima, I., Yoneda, N., Zimmer, A. & Kano, M. (2002) Presynaptic cannabinoid sensitivity is a major determinant of depolarization-induced retrograde suppression at hippocampal synapses. *J. Neurosci.*, **22**, 3864–3872.

Patricelli, M.P., Lashuel, H.A., Giang, D.K., Kelly, J.W. & Cravatt, B.F. (1998) Comparative characterization of a wild type and transmembrane domain-deleted fatty acid amide hydrolase: identification of the transmembrane domain as a site for oligomerization. *Biochemistry*, **37**, 15177–15187.

Rodriguez de Fonseca, F., Navarro, M., Gomez, R., Escuredo, L., Nava, F., Fu, J., Murillo-Rodriguez, E., Giuffrida, A., LoVerme, J., Gaetani, S., Kathuria, S., Gall, C. & Piomelli, D. (2001) An anorexic lipid mediator regulated by feeding. *Nature*, **414**, 209–212.

Shen, M., Piser, T.M., Seybold, V.S. & Thayer, S.A. (1996) Cannabinoid receptor agonists inhibit glutamatergic synaptic transmission in rat hippocampal cultures. *J. Neurosci.*, **16**, 4322–4334.

Sloviter, R.S. (1989) Calcium-binding protein (calbindin-D28k) and parvalbumin immunocytochemistry: localization in the rat hippocampus with specific reference to the selective vulnerability of hippocampal neurons to seizure activity. *J. Comp. Neurol.*, **280**, 183–196.

Stella, N. & Piomelli, D. (2001) Receptor-dependent formation of endogenous cannabinoids in cortical neurons. *Eur. J. Pharmacol.*, **425**, 189–196.

Stella, N., Schweitzer, P. & Piomelli, D. (1997) A second endogenous cannabinoid that modulates long-term potentiation. *Nature*, **388**, 773–778.

Szabat, E., Soinila, S., Happola, O., Linnala, A. & Virtanen, I. (1992) A new monoclonal antibody against the GABA-protein conjugate shows immunoreactivity in sensory neurons of the rat. *Neuroscience*, **47**, 409–420.

Thomas, E.A., Cravatt, B.F., Danielson, P.E., Gilula, N.B. & Sutcliffe, J.G. (1997) Fatty acid amide hydrolase, the degradative enzyme for anandamide and oleamide, has selective distribution in neurons within the rat central nervous system. *J. Neurosci. Res.*, **50**, 1047–1052.

Tsou, K., Brown, S., Sanudo-Pena, M.C., Mackie, K. & Walker, J.M. (1998a) Immunohistochemical distribution of cannabinoid CB1 receptors in the rat central nervous system. *Neuroscience*, **83**, 393–411.

Tsou, K., Nogueron, M.I., Muthian, S., Sanudo-Pena, M.C., Hillard, C.J., Deutsch, D.G. & Walker, J.M. (1998b) Fatty acid amide hydrolase is located preferentially in large neurons in the rat central nervous system as revealed by immunohistochemistry. *Neurosci. Lett.*, **254**, 137–140.

Wilson, R.I. & Nicoll, R.A. (2001) Endogenous cannabinoids mediate retrograde signalling at hippocampal synapses. *Nature*, **410**, 588–592.